International Journal of Engineering Research & Technology (IJERT)
ISSN: 2278-0181
Vol. 6 Issue 03, March-2017

Development of Operating Envelopes for Drillpipes Running through Medium to High Curvature Wells

A. C. Seibi[1*], R. Trabelsi[1], F. Boukadi[1]
[1]University of Louisiana,
Department of Petroleum Engineering
Lafayette, Louisiana, USA

T. Pervez[2],
[2]Sultan Qaboos University,
College of Engineering Mechanical Engineering
Department, P.O. Box 33
Al-Khod 123, Oman

M. Al-Khozaimi[3],
[3]Petroleum Development Oman
P.O. Box 33, Mina El-Fahl 123, Oman

Abstract **- The present paper aims at establishing elastic/plastic operating envelopes of drillpipes running through medium to high curvature wellbores. The operating envelopes will serve as guidelines for drilling engineers by identifying the operating limits of various API drillpipes used in curved wells before undergoing any activities. A two-dimensional mathematical model, which incorporates various field parameters that affect the running operation in medium to high curvature boreholes, has been developed. The developed model is capable of studying the effect of the vertical force at the kick off point (k.o.p), the back push (horizontal) force at the end of curve (e.o.c), radius of curvature, drillpipe bending stiffness, and formation roughness on the running operation. Two boundary conditions (fixed-fixed and pinned-pinned) at both ends of the drillpipes (k.o.p and e.o.c) were treated. The developed model estimates the required running force as well as the induced stresses of potential API drillpipes in curved well bores. The stress state, in drillpipes running through curved sections, was used to develop operating envelopes for drillpipes running through typical well configurations. The model also enables field engineers to select appropriate drillpipes according to operating field conditions in order to avoid any unexpected failure.**

INTRODUCTION

Directional drilling is commonly used to reach lateral targets within oil and gas reservoirs. Current directional drilling technology provides the capability to drill, navigate and control hole paths along a predetermined well path. Mechanical friction between drillpipes and wellbore presents a major concern in directional drilling because it i) increases the surface power required to rotate the drillpipe, ii) may cause drillpipes to get stuck to the formation making it difficult or impossible to pull out of the borehole; and iii) makes it difficult to establish and estimate a given weight on drillbits while drilling.

In horizontal drilling, the build-up section represents the most critical part of the drilling operation. Available literature published in the past presented different models to predict the behavior of drillpipes running through curved holes [1 – 11]. Of particular importance to this subject is the work done by Seibi et al. [9 – 12] and Martinez et al. [13] who conducted experimental and numerical studies on pipes running through curved holes and concluded that the end forces are affected by the contact between the pipe and formation due to lateral pipe deformation. These studies were further investigated experimentally by Kuru et al. [14] to study the effect of buckling on the axial force and concluded that i) the end support conditions of the tubular have a significant effect on tubular buckling, and ii) tubular buckling controls the contact force, and hence, the axial force. Most of the existing models do not consider the effect of various parameters affecting the stress state in drillpipes while running through curved sections. These parameters such as drag force, drillpipe weight, drillpipe bending stiffness, and borehole curvature may limit the extension of horizontal wells. Prediction of drag forces as well as bending moments play a great role in moving from vertical to horizontal drilling because it assists drilling engineers in designing well paths with appropriate radii of curvatures and selecting appropriate weights on bits to avoid any unexpected failure. Although extensive lab, field, and simulation work dealing with this problem has been performed, none has considered the operating limits of drillpipes running through curved sections. Therefore, the present paper focuses on the development of a mathematical model capable of establishing elastic/plastic working envelopes through careful examination of the induced stress state in drillpipes running through deviated wells.

MATHEMATICAL MODEL

The problem of drillpipes running through curved sections was modeled as a multi-span simply supported beam where two cases of boundary conditions at both ends of the curved sections were treated. Fixed-fixed and pinned-pinned boundary conditions at the k.o.p and e.o.c of the curved sections were considered. Figure A.1 shows the free body diagram of an infinitesimal element of a running drillpipe through a curved section from which equilibrium equations

International Journal of Engineering Research & Technology (IJERT)
ISSN: 2278-0181
Vol. 6 Issue 03, March-2017

were obtained. The governing equation of an infinitesimal element of a drillpipe running through curved boreholes is given by:

$$\frac{d^2M}{ds^2}+\frac{dV}{ds}+P\frac{d^2w}{ds^2}=0 \tag{1}$$

where *M*, *V*, *P*, and *w* denote respectively the bending moment, shear force, compressive normal force, and drillpipe radial deflection. In this model, the normal force was assumed to be constant throughout each span. Using the definition of the total curvature of the beam defined by $\frac{1}{\rho}=\frac{1}{R}+\frac{w}{R^2}+\frac{d^2w}{ds^2}$ and assuming Euler's beam bending yields to the following fourth order differential equation:

$$\frac{d^4w}{ds^4}+\left(\frac{1}{R^2}+\frac{P}{EI}\right)\frac{d^2w}{ds^2}=\frac{1}{EI}\left(q-\frac{P}{R}\right) \tag{2}$$

Solution of Equation (2) is given by:

$$w(s)=As+B+C\cosh\lambda s+D\sinh\lambda s-\frac{1}{2}\chi s^2 \tag{3}$$

Since the curved drillpipe was divided into many small elements, solution of Equation (2) was performed in multi-steps using the transfer matrix method. The constants of integration were obtained from the boundary conditions at the free ends (k.o.p and e.o.c) of the curved drillpipe. Using the assigned values of the drillpipe deflection and slope, Equation (3) and its derivative lead to the following general form (see Appendix):

$$M_1=\frac{\phi_{n+1}-(\gamma_{11})_{n+1}\phi_1-(\delta_{11})_{n+1}}{(\gamma_{12})_{n+1}}$$

$$\phi_1=\frac{M_{n+1}-(\gamma_{22})_{n+1}M_1-(\delta_{21})_{n+1}}{(\gamma_{21})_{n+1}} \tag{4}$$

$$M_{n+1}=(\gamma_{21})_{n+1}\phi_1+(\gamma_{22})_{n+1}M_1+(\delta_{21})_{n+1}$$

$$\phi_{n+1}=(\gamma_{11})_{n+1}\phi_1+(\gamma_{12})_{n+1}M_1+(\delta_{11})_{n+1} \tag{5}$$

Equations (4) and (5) represent respectively the bending moment and slope at the beginning ($\theta=0^o$, k.o.p) and end of drillpipe ($\theta=90^o$, e.o.c). The developed mathematical model is capable of predicting the reaction force at the contact points, compressive forces at the k.o.p, and stress distribution in each drillpipe span. The magnitude of compression in the top span (k.o.p) represents the force required to push the tubular through 90-deg curved borehole sections.

SOLUTION METHOD

The transfer matrix method was used to solve the problem of multi-span simply supported beams representing a typical drillpipe running through 90 degrees curved sections. A computer program was developed to estimate the compressive force, radial displacement, shear force, and induced stresses along the multi-span curved drillpipe. Table 1 shows the main steps involved in solving this problem. It is worth noting that results of the preceding sections are used to solve for the adjacent sections.

Table 1: Flowchart of the solution procedure

Step	Process
1	• Input desired load on the bit (P_0), radius of curvature (R), size and modulus of elasticity of drillpipe, coefficient of Coulomb friction between drillpipe and borehole (μ).
2	• Calculate body forces on each section.
3	• Initiate an iterative loop to calculate the following parameters (Appendix): λ_i, ζ_i, χ_i, ψ_i, $\lfloor\beta\rfloor_i$, $\lfloor\alpha\rfloor_i$, $\{a\}_i$, $\{b\}_i$, $[\gamma]_1$, and $\{\delta\}_1$ ➔ calculate $[\gamma]_{i+1}$ and $\{\delta\}_{i+1}$
4	• For a given end condition (fixed-fixed or simply supported boundary conditions at the k.o.p and e.o.c) use (4) to estimate bending moment and slope at first support of the first span.
5	• Calculate all ϕ_i and M_i.
6	
7	• Compute all constants C_i, D_i, B_i, and A_i
8	• Calculate deflection, slope, moment, and shear force on any section. • Using known internal shear forces at the beginning and the end of each section, update normal reactions Q_i at each support. For i =1 $Q_1=V_1$ at first span Calculate P_1 using (A.39) for a given weight on bit P_0 For i =2, 3, …, $n+1$

International Journal of Engineering Research & Technology (IJERT)
ISSN: 2278-0181
Vol. 6 Issue 03, March-2017

9 10	$Q_i = V_i - V_{i-1}$ V_i : shear force at the beginning of the span V_{i-1} : shear force at the end of the span • Calculate all new values of P_i using Eq. (A.39) • Compare new values of P_i obtained in step 9 with values of P_i estimated in steps 4 to 8 until convergence is achieved with ± 1 kN accuracy.

RESULTS AND DISCUSSION:

The effect of bending stiffness (EI), formation roughness, radius of curvature, and required back push force caused by drag force in the horizontal section on the running forces, are studied. Different case studies were used to predict the running force and induced stresses of drillpipes running through medium to high curvature borehole sections (see Table 2). The mechanical properties of selected API grade drillpipes are summarized in Table 3. In the model, the drillpipe was divided into multi-sections (spans) of 5° arc angle. The number of sections depends on the radius of curvature of curved sections. Two different boundary conditions at both ends of the drillpipe consisting of: 1) fixed-fixed drillpipe ends and 2) pinned-pinned drillpipe ends were considered.

Table 2: Drillpipes dimensions used in this study

Drill drillpipes size inches (mm)	Drill drillpipes Weight lbf/ft (N/m)	Grade	Radius of curvature (m)	Friction Coefficient μ
2 3/8 (60.3)	4.85 (70.8)	X	10, 25, 50, 75, 100, 200	0.1, 0.2, 0.3, 0.4
3 ½ (88.9)	13.3 (194)	E & X	10, 25, 50, 75, 100, 200	0.1, 0.2, 0.3, 0.4
4 ½ (114.3)	16.6 (242)	E & X	10, 25, 50, 75, 100, 200	0.1, 0.2, 0.3, 0.4
5 (127.0)	19.5 (285)	E	10, 25, 50, 75, 100, 200	0.1, 0.2, 0.3, 0.4

Table 3: Mechanical properties of API grade drillpipes

Grade	Ultimate tensile strength (MPa)	Yield strength (MPa)	Modulus of elasticity (GPa)
E-75	689	517	207
X-95	724	655	207
G-105	793	724	207
S-135	1000	931	207

The effect of formation roughness on the running force was studied for four different values of coefficient of friction, 0.1, 0.2, 0.3, and 0.4, using a drillpipe (bending stiffness EI of 3.87 x 10^5 Nm^2) under fixed-fixed boundary condition. A radius of curvature of 200 m and a load on bit of 20 kN are arbitrarily selected. The relationship between the running force and the inclination angle for different coefficients of friction is shown in Figure 1. It is obvious that as the coefficient of friction increases, the running force required to pushing the drillpipe increases. Variation in magnitude of the running force increases as the inclination angle increases and exhibit a nonlinear behavior. This means that the formation roughness or drag force is one of the key factors in affecting the running process and should be carefully considered in any drilling operation. Figure 2 shows the effect of formation roughness on drillpipe bending stress. It can be seen that the bending stress exhibits a reversed sign ranging from positive to negative peaks as the drillpipe moves forward. This stress variation is observed for all coefficients of friction. It is worth mentioning that for low friction coefficient ($\mu < 0.3$), the peak values of the bending stress is below the yield stress of the selected API drillpipes (see Table 2). However, the stress value exceeds the yield stress of the drillpipes for higher coefficients friction ($\mu > 0.3$) and becomes severe starting from an inclination angle of 65 degrees. This variation of stress and increase in its magnitude can be the result of a combination of factors related to the dogleg severity along the well path and tubular buckling in curved sections where the stress variation takes sinusoidal shapes due to high friction force as indicated by Wu and Wold [15]. Thereby, when the drillpipe buckles in a sinusoidal shape the bending stress becomes compressive and tensile along the curved section. This may lead to the possibility of drillpipes fatigue failure in all cases.

International Journal of Engineering Research & Technology (IJERT)
ISSN: 2278-0181
Vol. 6 Issue 03, March-2017

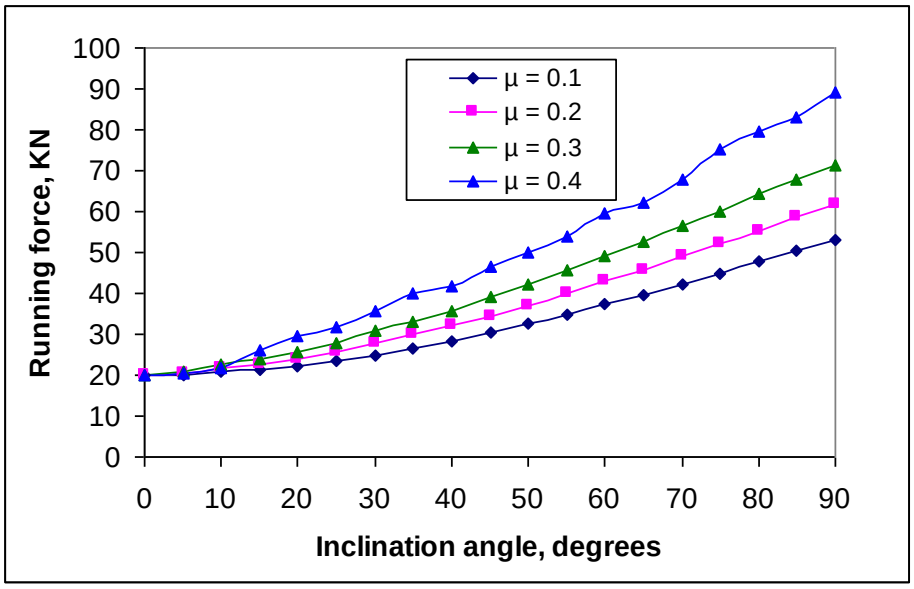

Fig. 1: Effect of formation roughness on running force

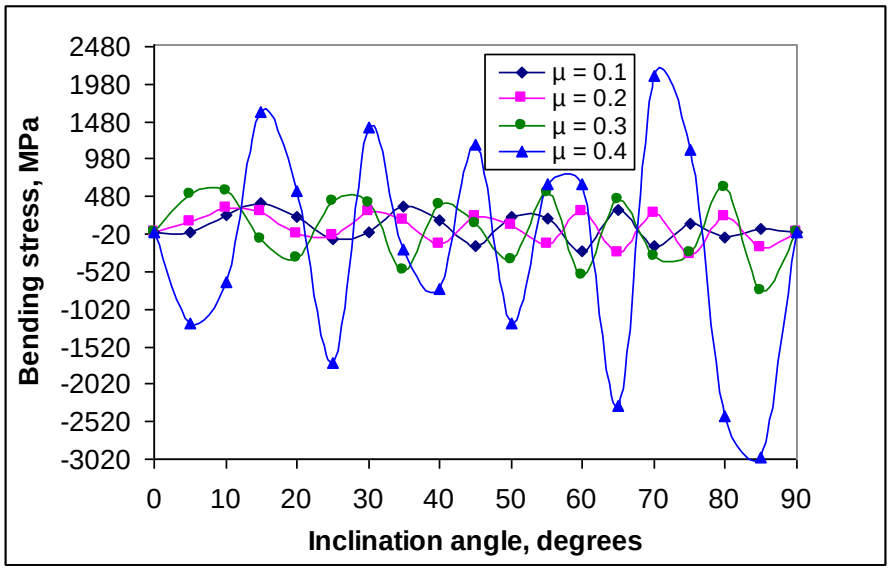

Fig. 2: Effect of formation roughness on bending stress

Another important parameter that has significant effects on the drillpipe stress state is the drillpipe weight/size (bending stiffness, EI). Four different drillpipes specific weights of 70.8, 194, 242, and 285 N/m under fixed-fixed boundary conditions were considered. These drillpipe sizes were arbitrarily chosen giving a range of drillpipes bending stiffnesses of 6.71 x 10^4, 3.87 x 10^5, 8.26 x 10^5, and 1.23 x 10^6 Nm^2. A radius of curvature of 50 m and a friction coefficient of 0.2 which provides low stress level as compared to the yield stress of the drillpipes were selected to study the effect of drillpipe bending stiffness on running forces. A load of 30 kN was applied at the bit. Figure 3 shows the variation of the running force as a function of the inclination angle. It can be seen that the vertical (running) force increases as the weight of the drillpipe increases implying that the higher the drillpipe bending stiffness, the higher the running force. The figure also shows that the running force is very low for all drillpipe sizes up to an inclination angle of 40 degrees beyond which the force starts to level off to much higher values. This increase in the running force becomes more apparent as the drillpipe bending stiffness gets higher. However, for low drillpipe bending stiffness, the running force is very low and does not exhibit any variation with respect to the inclination angle. This behavior was observed by Seibi [11]. This suggests the use of the cable model for this particular case, which neglects the effect of drillpipe bending stiffness. Further advancement of drillpipes along the curved section results in excessive induced bending stresses. Figure 4 shows the variation of the bending stress versus the inclination angle for different drillpipe sizes. It can be observed that drillpipes of high specific weights experience high alternating bending stresses, which exceed the yield stress of the drillpipes, for inclination angles higher than 30 degrees. This increase in stress level may be due to excessive compressive force at the end of curve which is much higher than the critical buckling force in curved [15] which may lead to sinusoidal or helical buckling modes;

International Journal of Engineering Research & Technology (IJERT)
ISSN: 2278-0181
Vol. 6 Issue 03, March-2017

thereby, leading to cyclic stress variation. This indicates that there is a very high chance for fatigue failure to take place; thereby, careful selection of drillpipes before undergoing any activity must be performed.

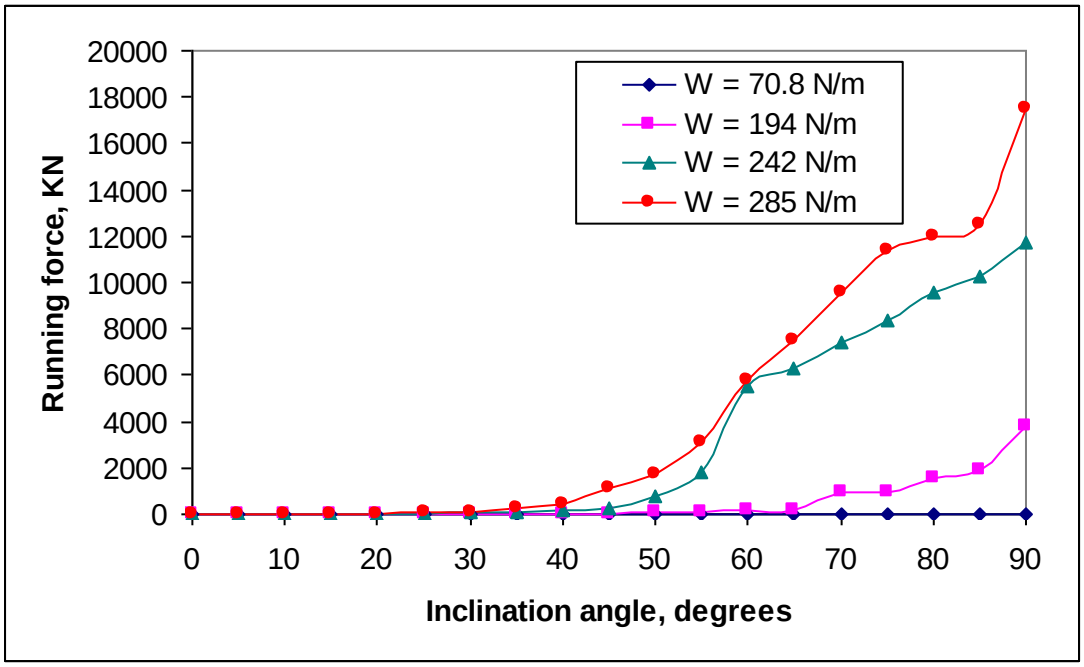

Fig. 3: Effect of bending stiffness on running force

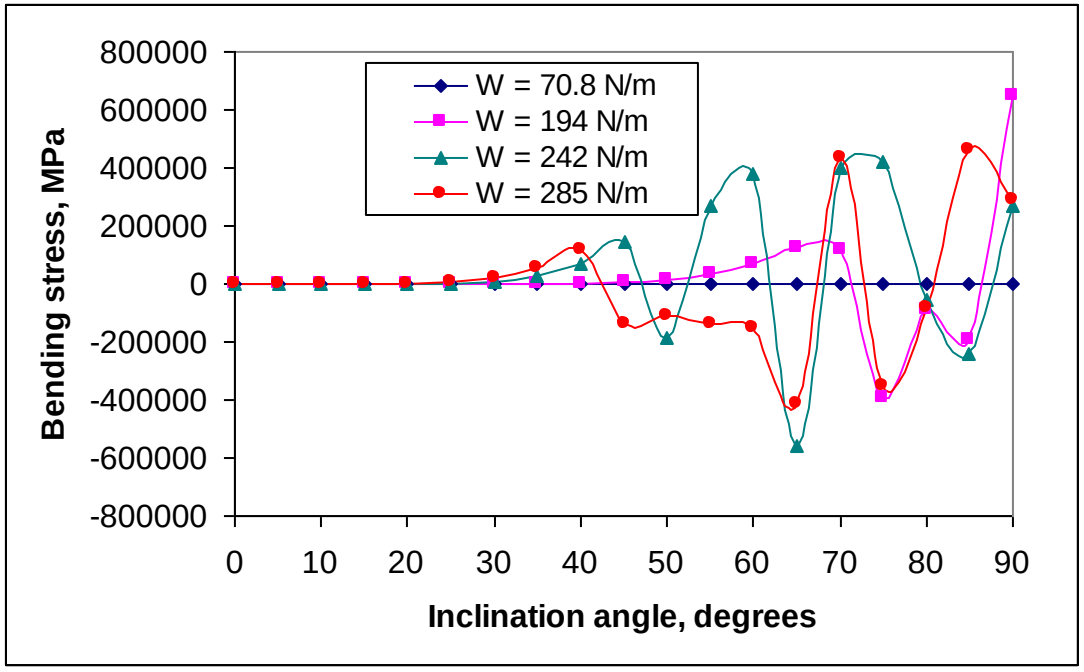

Fig. 4: Effect of bending stiffness on bending stress

The effect of the radius of curvature of curved hole sections on the running force is studied by considering three radii of curvatures i.e. 50, 100, and 200 m. The developed model was used to calculate the running forces for a drillpipe running through the build-up section. The drillpipes used in this case has respectively an outer and inner diameter of 0.0603 and 0.0507 m and a specific weight of 70.8 N/m under fixed-fixed boundary conditions. The other field parameters such as friction coefficient, mud density, and load on bit were given constant values of 0.3, 198 Kg/m^3, and 10 kN, respectively. Figure 5 shows the instantaneous vertical (running) force required to push the drillpipes through high to medium curvature wellbores (50, 100, and 200 m). It can be observed that the running force at the k.o.p increases as the radius of curvature decreases. A substantial increase in the vertical force is observed for a radius of curvature of 50 m as compared to the other two radii of curvatures. The running force is almost the same for all radii of curvatures up to an inclination angle of 40 degrees. For instance, for the case of a radius of curvature of 50 m, the running force starts to increase gradually between 40 – 50 degrees and exhibits a sharp increase beyond the 50 degrees inclination angle. This increase in magnitude is mainly related to the increase in drag forces at

International Journal of Engineering Research & Technology (IJERT)
ISSN: 2278-0181
Vol. 6 Issue 03, March-2017

contact points indicating that the total force required to push the drillpipe (OD = 0.0603 m) through curved wells is highest for holes with shorter radii of curvatures (R < 50 m) and lowest for higher radii of curvatures (R > 200 m). This phenomenon is mainly attributed to wellbore curvature and drillpipe bending stiffness effects which become prominent for short curvature wellbores (severe doglegs). However, the small increase in the running force for both radii of curvatures of 100 and 200 m within the first 60 degrees is mainly attributed to the drillpipe weight which is acting in the same direction as the running force. Therefore, the weight in these two cases helps the drillpipe advance further downward along the curved hole. However, for inclination angles exceeding 60 degrees, a slight increase in the running force is observed for both radii of curvatures as a result of further resistance caused by drag forces.

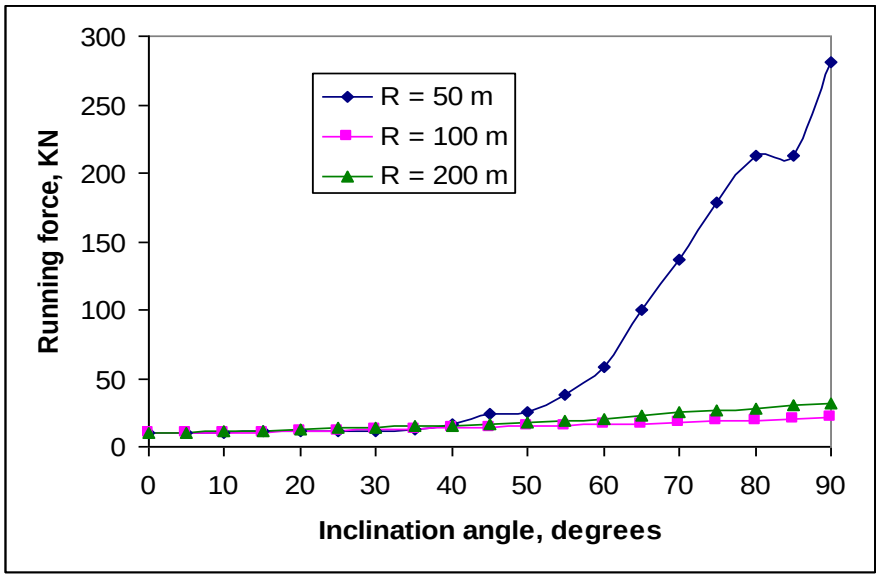

Fig. 5: Effect of radius of curvature on running forces

The induced bending stress in the drillpipe running through the three radii of curvatures is shown in Figure 6. The figure shows that the drillpipe experiences an alternating high bending stress as it advances through short radii of curvatures (R < 50 m). This phenomenon is attributed to the high compressive force at the end of curve cuasing pipe buckling as well as pipe bending stiffness which requires a much high stress level to bend the drillpipe and follow the curved path. This observation was made by Seibi [12] where pipe bending becomes more apparent for high curvature wellbores. Similar observations can be made for the radius of curvature of 200 m but with less severity. The high stress values may lead to unexpected drillpipe failure. It is worth mentioning that the compressive force in the drillpipe was observed to increase with respect to the inclination angle as it advances from the build up point to the end of curve. This phenomenon was observed by Dareing [4] for a pullout operation where the pullout force increases with respect to the inclination angle.

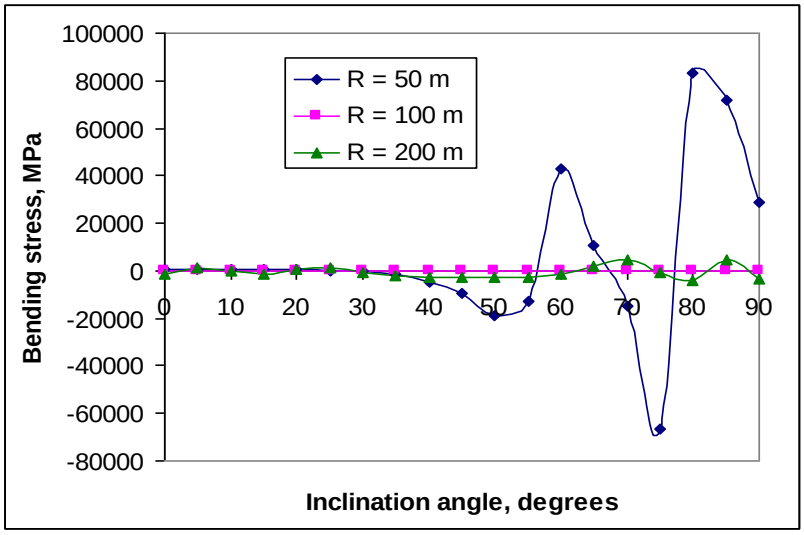

Fig. 6: Effect of radius of curvature on bending stress

International Journal of Engineering Research & Technology (IJERT)
ISSN: 2278-0181
Vol. 6 Issue 03, March-2017

Working Envelope for Drillpipes under Running Operations

This section aims at providing drilling engineers with proper guidelines that predetermine the possibility of running drillpipes through curved sections without undergoing any plastic deformation. These guidelines are presented in the form of a working envelope that was developed based on the induced stress levels in drillpipes. In other words, the induced normal stress caused by drillpipes bending and axial loads was compared against the yield stress of various API drillpipes. The criterion adopted in this study was based on stress values higher than the yield stress indicating that drillpipes undergo plastic deformation which may result in drillpipes buckling or sticking to the formation. Based on this hypothesis, a working envelope was developed for various field cases to aid drilling engineers in i) selecting suitable drillpipes as per field operating conditions in order to avoid any unexpected failure and ii) making sound decisions while developing well paths before undergoing any drilling activities.

The aforementioned results related to the effect of drillpipes bending stiffness, radius of curvature, wellbore curvature, coefficient of friction, and boundary conditions were used to develop the failure/operating envelop. The parameters used in this study are summarized in Table 4.

Table 4 Parametric matrix used in this study

Wob kN	Radius of curvature (m)	Drillpipe weight (N/m)	Friction coefficient
10	10	78.8	0.1
15	25	194	0.2
20	50	242	0.3
25	75	285	0.4
30	100		
	200		

Table 5 shows the obtained results for various field scenarios where shaded areas indicate that drillpipes can safely run through the curved holes for particular field cases without undergoing any plastic deformation. Whereas, the unshaded areas indicate that drillpipe failure may take place since the induced stresses on the drillpipes exceed the yield stress. For instance, a drillpipe with a specific weight of 70.8 N/m can be ran without any problem into a well having a radius of curvature of 100 m and a load on bit of 10 kN with a coefficient of friction of 0.4; while a drillpipe with a specific gravity of 194 N/m cannot run safely. The table also shows that drillpipes of 242 N//m and 285 N/m cannot be safely run into curved wells at all selected field conditions when a 10 kN load on bit is applied. Similar observations can be made in the case of pinned-pinned boundary conditions.

CONCLUSIONS

The major steps in developing a two-dimensional mathematical model based on Dareing and Ahlers model were described in details. Various field parameters that affect the drillpipes in build-up sections, such as coefficient of friction, radius of curvature, and bending stiffness, were incorporated in the developed model. Calculations show that the soft string model used to determine the running force is an approximation method provided that there are no severe local doglegs within the build-up section. It was also found that the running force increases as the inclination angle, coefficient of friction, drillpipe bending stiffness, and radius of curvature increase along the build-up section. Moreover, a useful operating envelope for various drillpipe sizes and field conditions was developed. This envelope is a useful tool to field engineers during well planning phase.

REFERENCES

[1] Birades M., 1988, “Static and Dynamic Three-Dimensional BHA Computer Models,” SPE Paper No. 15466, SPE Drilling Engineering, Vol. 3, 2, pp: 160 – 166.

[2] Dareing D.W. and Ghodwani S., 1970, “Directional Drilling and Circular Arc Deflection of Long Beam,” SPE Paper No. 3097, Meeting of the Society of Petroleum Engineers of AIME, 4 – 7 Oct., Houston, Texas.

[3] Dareing D.W., 1971, “Drilling Directional Holes Having Constant Curvature,” SPE Paper No. 3508, Meeting of the Society of Petroleum Engineers of AIME, 4 – 7 Oct., Houston, Texas.

[4] Dareing D.W. and Ahlers C.A, 1991, "Tubular Bending and Pull-Out Forces in High-Curvature Wellbores,” Journal of Energy Resources Technology, Vol.113, pp.133-139.

[5] Haduch G.A, Procter R.L. and Samuels D.A., 1994, "Solution of Common Stuck Drillpipes Problems through the Adaptation of Torque/Drag Calculations,” SPE Paper No. 27490, SPE/IADC Drilling Conference 15 – 18 February, Dallas, Texas.

[6] Ho H-S., 1988, “An Improved Modeling Program for Computing the Torque and Drag in Directional and Deep Wells,” SPE Paper No. 18047, SPE Annual Technical Conference & Exhibition, 2 – 5 October, Houston, Texas.

[7] Johancsick C.A., Friesen D. B. and Dawson R., 1984, “Torque and Drag in Directional Wells-Predictions and Measurement,” SPE Paper No. 11380, J. of Petroleum Technology, Vol.36, 6, pp: 987 – 992.

[8] Paslay P.R. and Cernocky E.P., 1991, “Bending Stress Magnification in Constant Curvature Doglegs With Impact on Drillpipes and Drillpipes,” SPE Paper No. 22547, SPE Annual Technical Conference & Exhibition, 6 – 9 October, Dallas, Texas.

[9] Seibi A.C., 2000, “Running Force Measurement in High Curvature Wellbores," *Journal of Experimental Techniques*, March/April, pp. 31-35.

International Journal of Engineering Research & Technology (IJERT)
ISSN: 2278-0181
Vol. 6 Issue 03, March-2017

[10] Seibi A.C. and Al-Hashmi M.A., 1998, "Effects of Drillpipes/Formation Interaction on The Running Force in High-Curvature Wellbores," ASME/JSME Joint Pressure Vessels and Piping Conference, San Diego, CA, July 26-30, PVP- Vol. 375, pp. 89-94.

[11] Seibi, A.C. and Al-Shabibi, A.M., 1998, "Drillpipes Bending and Running Forces in Medium to High Curvature Wells Using Finite Element Analysis," Journal of Energy Resources Technology, Vol.120, pp. 263-267.

[12] Seibi, A., 2001, "Running Force in Medium to High-Curvature Wellbores: An Experimental Study and Numerical Simulation of Laboratory and Field Cases," Journal of Energy Resources Technology, Vol. 123, pp: 133 – 137.

[13] Martinez, A., Miska, S., Kuru, E., Sorem, J., 2000, "Experimental Evaluation of the Lateral Contact Force in Horizontal Wells," Journal of Energy Resources Technology, Vol. 122, pp: 123 – 128.

[14] Kuru, E., Martinez, A., Miska, S., Qiu, W., 2000, "The Buckling Behavior of Pipes and Its Influence on the Axial Force Transfer in Directional Wells," Journal of Energy Resources Technology, Vol. 122, pp: 129 – 135.

[15] Wu, J., Juvkam Wold, H. C., "The Effect of Wellbore Curvature on Buckling and Lockup," J. of Energy Resources Technology, Vol. 117, pp: 214 – 218.

APPENDIX

Governing Equations of Drillpipes Running Through Curved Sections

The governing equations are derived by considering the equilibrium of an infinitesimal element of a drilldrillpipes running through curved boreholes. Figure A.1 shows a free body diagram of a differential element under compression. The drilldrillpipes was modeled as a multi-span simply supported beam with multiple supports representing contact between the drilldrillpipes and borehole walls starting from the kick-off point till the end of curve.

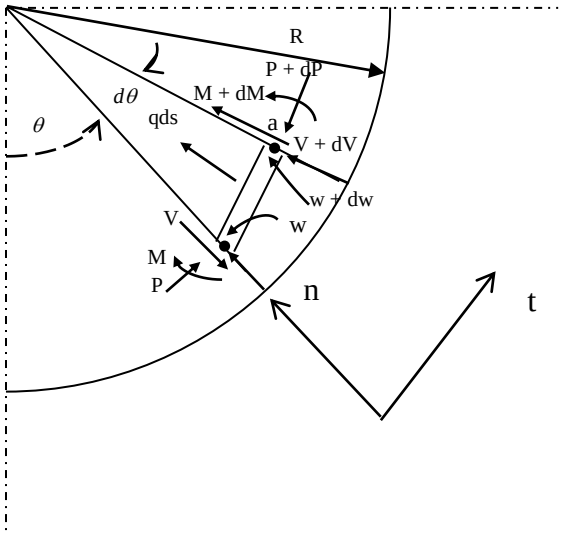

Fig. A.1: Free body diagram of differential element under compression in terms of polar coordinates

Using the equilibrium equation in the normal direction and neglecting higher order terms leads to the following first order of differential equation:

$$\frac{dV}{ds} = \left(-q + \frac{P}{R} \right) \qquad \text{(A.1)}$$

where, q is a distributed force per unit length.

Using the equilibrium equation of the moment about point **a** and neglecting the higher order terms, a first order differential equation is given by:

$$\frac{dM}{ds} + V + P\frac{dw}{ds} = 0 \qquad \text{(A.2)}$$

Differentiating equation (A.2) with respect to s leads to the following equation:

$$\frac{\mathrm{d}^2 M}{ds^2} + \frac{dV}{ds} + P\frac{d^2 w}{ds^2} = 0 \qquad \text{(A.3)}$$

Note that the dependent variable, w, is the radial displacement of the beam where positive displacement is taken in the inward direction. Considering the total curvature of the beam in terms of polar coordinates defined by $\frac{1}{\rho} = \frac{1}{R} + \frac{w}{R^2} + \frac{d^2 w}{ds^2}$ and assuming Euler Bending, the bending moment takes the form:

$$M = EI\left[\frac{1}{R} + \frac{w}{R^2} + \frac{d^2 w}{ds^2} \right] \qquad \text{(A.4)}$$

Differentiating Equation (A.4) with respect to s twice becomes,

International Journal of Engineering Research & Technology (IJERT)
ISSN: 2278-0181
Vol. 6 Issue 03, March-2017

$$\frac{d^2M}{ds^2} = EI\left[\frac{1}{R^2}\frac{d^2w}{ds^2} + \frac{d^4w}{ds^4}\right] \qquad \text{(A.5)}$$

Combining of Equations (A.1), (A.3), and (A.5) results in a fourth order differential equation in terms of radial displacement given by:

$$\frac{d^4w}{ds^4} + \lambda^2\frac{d^2w}{ds^2} = \zeta \qquad \text{(A.6)}$$

where,

$\lambda^2 = \left(\frac{P}{EI} + \frac{1}{R^2}\right)$ and $\zeta = \frac{1}{EI}\left(q - \frac{P}{R}\right) = \frac{Rq - P}{REI}$

The compressive force is assumed to be constant over a given section.

Solution Method

Solution to Equation (A.6) gives the deviation of the radial displacement of a drillpipes from the centerline of the target well path of a typical borehole and takes the following form:

$$w(s) = -\frac{1}{2}\chi_i s^2 + A_i s + B_i + C_i\cos(\lambda_i s) + D_i\sin(\lambda_i s) \qquad \text{(A.7)}$$

where, $\chi = \dfrac{-Rq + P}{RP + \dfrac{EI}{R}}$

Using the boundary conditions at the beginning of the ith section (where ith support is located, $s = 0$ and $w(0) = w_i$) in (A.7) gives:

$$w(0) = B_i + C_i = w_i \qquad \text{(A.8)}$$

Similarly, at the other end of the ith section (where the $(i+1)th$ support is located), $s = l_i$, and $w(l_i) = w_{i+1}$. Substituting these values in equation (A.7) gives:

$$w(l_i) = -\frac{1}{2}\chi_i {l_i}^2 + A_i l_i + B_i + C_i\cos(\lambda_i l_i) + D_i\sin(\lambda_i l_i) = w_{i+1} \qquad \text{(A.9)}$$

Substituting B_i from (A.8) into (A.9) and solving for A_i yields:

$$A_i = (\psi_i + \frac{1}{2}\chi_i l_i) - C_i\frac{(\cos(\lambda_i l_i) - 1)}{l_i} - D_i\frac{\sin(\lambda_i l_i)}{l_i} \qquad \text{(A.10)}$$

where, ψ_i is defined as $\psi_i = \dfrac{w_{i+1} - w_i}{l_i}$

The rate of change of w with respect to 's' is given by:

$$\phi = \frac{dw}{ds} = -\chi_i s + A_i - C_i\lambda_i\sin(\lambda_i s) + D_i\lambda_i\cos(\lambda_i s) \qquad \text{(A.11)}$$

Using equation (A.11), the slope at the beginning of ith section (at $s = 0$) can be calculated as:

$$\phi_i = A_i + D_i\lambda_i \qquad \text{(A.12)}$$

The bending moment at the beginning of the ith section is given by:

$$M_i = EI\left[\frac{1}{R} + \frac{w_i}{R^2} + \frac{d^2w_i}{ds^2}\right] \qquad \text{(A.13)}$$

Differentiating Equation (A.7) twice with respect to 's' and substituting s = 0 for ith point gives:

$$\frac{d^2w_i}{ds^2} = -\chi_i - C_i{\lambda_i}^2 \qquad \text{(A.14)}$$

Substituting Equation (A.8) and Equation (A.14) into Equation (A.13) results in:

International Journal of Engineering Research & Technology (IJERT)
ISSN: 2278-0181
Vol. 6 Issue 03, March-2017

$$M_i = EI\left[\frac{1}{R} + \frac{B_i + C_i}{R^2} - \chi_i - C_i\lambda_i^{\,2}\right] \tag{A.15}$$

Substituting A_i and B_i into (A.12) and (A.15), respectively, results in a simplified form for the slope and bending moment at the beginning of ith section:

$$\phi_{\mathrm{i}} = (\psi_i + \frac{1}{2}\chi_i l_i) + \left(\frac{(1-\cos(\lambda_i l_i))}{l_i}\right)C_i + \left(\lambda_i - \frac{\sin(\lambda_i l_i)}{l_i}\right)D_i \tag{A.16}$$

$$M_i = EI\left(\frac{1}{R} + \frac{w_i}{R^2} - \chi_i\right) - C_i\lambda_i^{\,2}EI \tag{A.17}$$

Solving equations (A.16) and (A.17) for the constants C_i and D_i gives:

$$\begin{Bmatrix} C_i \\ D_i \end{Bmatrix} = [\alpha]_i \left(\begin{Bmatrix} \phi_i \\ M_i \end{Bmatrix} - \{a\}_i \right) \tag{A.18}$$

where,

$$[\alpha]_i^{-1} = \begin{bmatrix} \dfrac{(1-\cos(\lambda_i l_i))}{l_i} & \lambda_i - \dfrac{\sin(\lambda_i l_i)}{l_i} \\ -\lambda_i^{\,2}EI & 0 \end{bmatrix} \tag{A.19}$$

and

$$\{a\}_i = \begin{bmatrix} \psi_i + \dfrac{1}{2}\chi_i l_i \\ EI\left(\dfrac{1}{R} + \dfrac{w_i}{R^2} - \chi_i\right) \end{bmatrix} \tag{A.20}$$

Similarly, at the end of the ith section when $s = l_i$, the slope at the $(i+1)th$ support is:

$$\phi_{i+1} = -\chi_i l_i + A_i - C_i\lambda_i \sin(\lambda_i l_i) + D_i\lambda_i \cos(\lambda_i l_i) \tag{A.21}$$

Substituting constant A_i into (A.21) and simplifying, Equation (A.21) becomes:

$$\phi_{\mathrm{i+1}} = -\frac{1}{2}\chi_i l_i + \psi_i + \left[\frac{(1-\cos(\lambda_i l_i))}{l_i} - \lambda_i \sin(\lambda_i l_i)\right]C_i + \left[\lambda_i \cos(\lambda_i l_i) - \frac{\sin(\lambda_i l_i)}{l_i} + \right]D_i \tag{A.22}$$

Equation (A.22) represents the slope at the end of ith section. Similarly, the bending moment at the end of ith section, when $s = l_i$ (at $(i+1)th$ support) can be expressed as:

$$M_{\,i+1} = \frac{\mathrm{EI}}{\mathrm{R}}\left(1 + \frac{\mathrm{w_{i+1}}}{\mathrm{R}} - \mathrm{R}\chi_{\mathrm{i}}\right) - \mathrm{C_i}\lambda_{\mathrm{i}}^{\,2}\mathrm{EI}\,cos(\lambda_{\mathrm{i}}\mathrm{l_i}) - \mathrm{D_i}\lambda_{\mathrm{i}}^{\,2}\mathrm{EI}\,sin(\lambda_{\mathrm{i}}\mathrm{l_i}) \tag{A.23}$$

Expressing equations (A.22) and (A.23) in a matrix form leads to:

$$\begin{Bmatrix} \phi_{i+1} \\ M_{i+1} \end{Bmatrix} = [\beta]_i \begin{Bmatrix} C_i \\ D_i \end{Bmatrix} + \{b\}_i \tag{A.24}$$

where,

International Journal of Engineering Research & Technology (IJERT)
ISSN: 2278-0181
Vol. 6 Issue 03, March-2017

$$[\beta]_i = \begin{bmatrix} \frac{(1-\cos(\lambda_i l_i))}{l_i} - \lambda_i \sin(\lambda_i l_i) & \lambda_i \cos(\lambda_i l_i) - \frac{\sin(\lambda_i l_i)}{l_i} \\ -EI\lambda_i{}^2 \cos(\lambda_i l_i) & -EI\lambda_i{}^2 \sin(\lambda_i l_i) \end{bmatrix} \quad \text{(A.25)}$$

and

$$\{b\}_i = \begin{bmatrix} \psi_i - \frac{1}{2}\chi_i l_i \\ \frac{EI}{R}\left(1 + \frac{w_{i+1}}{R} - R\chi_i\right) \end{bmatrix} \quad \text{(A.26)}$$

Substituting constants $\begin{Bmatrix} C_i \\ D_i \end{Bmatrix}$ from Equation (A.18) into Equation (A.24) gives:

$$\begin{Bmatrix} \phi_{i+1} \\ M_{i+1} \end{Bmatrix} = [\beta]_i [\alpha]_i \left(\begin{Bmatrix} \phi_i \\ M_i \end{Bmatrix} - \{a\}_i \right) + \{b\}_i \quad \text{(A.27)}$$

As can be seen from equation (A.27) , the slope and bending moment at the end of a span ($i+1$) can be expressed in terms of the slope and bending moment at the beginning of the span.
The generalized form of equation (A.27) can be written as:

$$\begin{Bmatrix} \phi_{i+1} \\ M_{i+1} \end{Bmatrix} = [\beta]_i [\alpha]_i [\gamma]_i \begin{Bmatrix} \phi_1 \\ M_1 \end{Bmatrix} + [\beta]_i [\alpha]_i \left(\{\delta\}_i - \{a\}_i \right) + \{b\}_i \quad \text{(A.28)}$$

where,

$$\begin{Bmatrix} \phi_i \\ M_i \end{Bmatrix} = [\gamma]_i \begin{Bmatrix} \phi_1 \\ M_1 \end{Bmatrix} + \{\delta\}_i, \quad i = 1,2,....,n+1 \quad \text{(A.29)}$$

and where γ_i and δ_i are the matrices and vectors of constants of order 2x2 and 1x2, respectively, which are updated during each load increment where the initial values are given by $[\gamma]_1 = \begin{bmatrix} 1 & 0 \\ 0 & 1 \end{bmatrix}$ and $\{\delta\}_1 = \begin{Bmatrix} 0 \\ 0 \end{Bmatrix}$. Rewriting Equation (A.28) as:

$$\begin{Bmatrix} \phi_{i+1} \\ M_{i+1} \end{Bmatrix} = [\gamma]_{i+1} \begin{Bmatrix} \phi_1 \\ M_1 \end{Bmatrix} + \{\delta\}_{i+1} \quad \text{(A.30)}$$

where,

$$[\gamma]_{i+1} = [\beta]_i [\alpha]_i [\gamma]_i \quad \text{(A.31)}$$

and

$$\{\delta\}_{i+1} = [\beta]_i [\alpha]_i \left(\{\delta\}_i - \{a\}_i \right) + \{b\}_i \quad \text{(A.32)}$$

If the multi-span is composed of n sections, the number of supports along the multi-span is $n+1$. Hence equation (A.29) will extend from 1 to $n+1$ and Equation (A.30) becomes:

$$\begin{Bmatrix} \phi_{n+1} \\ M_{n+1} \end{Bmatrix} = [\gamma]_{n+1} \begin{Bmatrix} \phi_1 \\ M_1 \end{Bmatrix} + \{\delta\}_{n+1} = = \begin{bmatrix} \gamma_{11} & \gamma_{12} \\ \gamma_{21} & \gamma_{22} \end{bmatrix}_{n+1} \begin{Bmatrix} \phi_1 \\ M_1 \end{Bmatrix} + \begin{Bmatrix} \delta_{11} \\ \delta_{21} \end{Bmatrix}_{n+1} \quad \text{(A.33)}$$

Equation (A.33) relates the slope and bending moment at the two ends of the multi-span. *If* ϕ_1 and ϕ_{n+1} are given as end constraints, the bending moments at the two ends of the multi span can be obtained using following equations:

$$M_1 = \frac{\phi_{n+1} - (\gamma_{11})_{n+1}\phi_1 - (\delta_{11})_{n+1}}{(\gamma_{12})_{n+1}} \quad \text{(A.34)}$$

$$M_{n+1} = (\gamma_{21})_{n+1}\phi_1 + (\gamma_{22})_{n+1}M_1 + (\delta_{21})_{n+1} \quad \text{(A.35)}$$

Equation (A.34) represents the bending moment at the beginning of the tubular ($\theta = 0^o$) and Equation (A.35) represents the bending moment at the end of the tubular ($\theta = 90^o$) and vice versa. *If* M_1 and M_{n+1} are given as end constraints, the slopes at the two ends of the tubular are given by:

International Journal of Engineering Research & Technology (IJERT)
ISSN: 2278-0181
Vol. 6 Issue 03, March-2017

$$\phi_1 = \frac{M_{n+1} - (\gamma_{22})_{n+1} M_1 - (\delta_{21})_{n+1}}{(\gamma_{21})_{n+1}} \quad \text{(A.36)}$$

$$\phi_{n+1} = (\gamma_{11})_{n+1} \phi_1 + (\gamma_{12})_{n+1} M_1 + (\delta_{11})_{n+1} \quad \text{(A.37)}$$

Equations (A.36) and (A.37) represent the slope at the beginning of tubular ($\theta = 0^o$) and at the end of tubular ($\theta = 90^o$), respectively.

Compression over a given span

The assumption of a constant compressive force throughout a given section simplifies the undertaken problem while obtaining realistic engineering results. Figure A.2 shows the forces on a given span. The reaction force, Q_i, and the compressive force, P_i, at the ith support were determined from the equilibrium conditions.

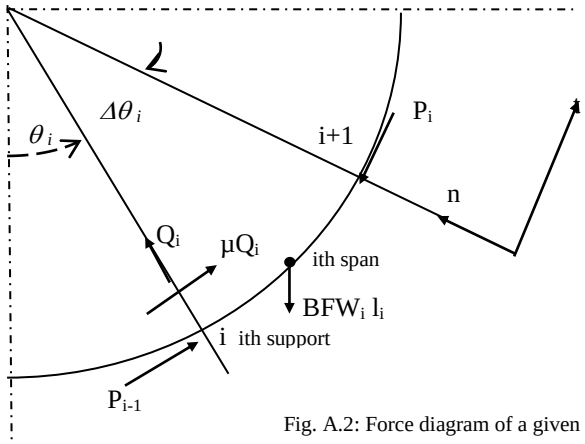

Fig. A.2: Force diagram of a given span

Summation of forces in the normal direction gives the reaction and compressive forces, respectively:

$$Q_i = \frac{P_{i-1} \sin(\Delta\theta_i) + BFW_i l_i \cos(\theta_i + \Delta\theta_i)}{\cos(\Delta\theta_i) - \mu \sin(\Delta\theta_i)} \quad \text{(A.38)}$$

Summation forces in the tangential direction gives:

$$P_i = (P_{i-1} + \mu |Q_i|) \cos(\Delta\theta_i) + Q_i \sin(\Delta\theta_i) + BFW_i l_i \sin(\theta_i + \Delta\theta_i) \quad \text{(A.39)}$$

where, P_0 is the load applied at the bit. The body force is estimated by the following expression:

$$q_i = -BFW_i \cos\left(\theta_i + \frac{\Delta\theta_i}{2}\right) \quad \text{(A.40)}$$

International Journal of Engineering Research & Technology (IJERT)
ISSN: 2278-0181
Vol. 6 Issue 03, March-2017

Table 5 Parameters for safe running operation for drillpipes with different specific weights and at various field conditions

Weight (N/m) / Back Pull N	70.8							194							242							285						
	R / μ	10	25	50	75	100	200	R / μ	10	25	50	75	100	200	R / μ	10	25	50	75	100	200	R / μ	10	25	50	75	100	200
10000	0.1					■		0.1						■	0.1							0.1						
	0.2					■		0.2							0.2							0.2						
	0.3					■		0.3							0.3							0.3						
	0.4					■		0.4							0.4							0.4						
15000	0.1					■		0.1						■	0.1							0.1						
	0.2				■	■		0.2						■	0.2							0.2						
	0.3				■	■		0.3						■	0.3							0.3						
	0.4				■	■		0.4							0.4							0.4						
20000	0.1				■	■		0.1						■	0.1							0.1						
	0.2				■	■		0.2						■	0.2							0.2						
	0.3				■	■		0.3							0.3						■	0.3						
	0.4				■	■		0.4							0.4							0.4						
25000	0.1				■	■		0.1						■	0.1							0.1						
	0.2				■	■		0.2							0.2						■	0.2						
	0.3				■	■		0.3							0.3						■	0.3						
	0.4				■			0.4							0.4						■	0.4						
30000	0.1				■	■		0.1						■	0.1						■	0.1						
	0.2			■	■	■		0.2							0.2						■	0.2						
	0.3			■	■	■		0.3							0.3							0.3						■
	0.4			■	■			0.4							0.4						■	0.4						■